

# Low-temperature methanol synthesis catalyzed over Cu/ $\gamma$ -Al<sub>2</sub>O<sub>3</sub>-TiO<sub>2</sub> for CO<sub>2</sub> hydrogenation

Gong-Xin Qi, Xiao-Ming Zheng\*, Jin-Hua Fei and Zhao-Yin Hou

*Institute of Catalysis, Zhejiang University (Xixi Campus), Hangzhou 310028, PR China*

Received 27 November 2000; accepted 18 January 2001

A titanium-modified  $\gamma$ -alumina-supported CuO catalyst has been prepared and used for methanol synthesis from CO<sub>2</sub> hydrogenation. XRD and TPR were used to characterize the phase, reduction property and particle size of the reduced catalyst. The addition of Ti to the CuO/ $\gamma$ -Al<sub>2</sub>O<sub>3</sub> catalyst made the copper in the catalyst exist in much smaller crystallites and exhibit an amorphous-like structure. The adding of Ti made the reduction peak shift toward lower temperature in comparison with the CuO/ $\gamma$ -Al<sub>2</sub>O<sub>3</sub> catalyst. The effect of the addition of Ti and the reaction conditions on the activity and selectivity to methanol from CO<sub>2</sub> hydrogenation were investigated. The activity was found to increase with increasing surface area of metallic copper, but it is not a linear relationship. This indicated that the catalytic activity of the catalysts depends on both the metallic copper area and the synergy between the copper and titanium dioxide. The effect of contact time on the relative selectivity ( $\kappa = S_{\text{CH}_3\text{OH}}/S_{\text{CO}}$ ) and selectivity of methanol were also investigated. The results indicated that methanol was formed directly from the hydrogenation of CO<sub>2</sub>.

**KEY WORDS:** CO<sub>2</sub> hydrogenation; methanol synthesis; Cu/ $\gamma$ -Al<sub>2</sub>O<sub>3</sub>-TiO<sub>2</sub>

## 1. Introduction

The methanol synthesis from carbon oxides and hydrogen over copper–zinc catalysts is usually operated above 250 °C and at a reaction pressure of more than 5.0 MPa. Because of the thermodynamic limitation, the yield of methanol is not high enough for the one-pass operation which is a breakthrough of the methanol production system. In order to realize it, the reaction must be carried out at 180 °C or less; however, under this condition, the utilization of an industrial Cu/ZnO/Al<sub>2</sub>O<sub>3</sub> catalyst, which exhibited a high activity for methanol synthesis from syngas, was not successful [1]. Recently, great efforts have been put into preparing an ideal catalyst for the hydrogenation of CO<sub>2</sub> [2–7]. Koppel and Baiker [2] studied the effect of the preparation method on the catalytic performance of Cu/ZrO<sub>2</sub> catalysts and found that the efficient catalyst consisted of microcrystalline copper particles which were stabilized through interaction with an amorphous matrix, leading to a high interfacial area. Satio et al. [3] investigated various metal oxides such as Ga<sub>2</sub>O<sub>3</sub>, Al<sub>2</sub>O<sub>3</sub>, ZrO<sub>2</sub> and Cr<sub>2</sub>O<sub>3</sub> contained in Cu/ZnO-based ternary catalysts and ascribed the high activity and stability of the catalyst to the improvement of Cu dispersion and the increase of specific activity by metal oxides. The catalytic activity of Cu-based catalysts depends on the properties of their supports. It is generally accepted that metals supported on reducible oxides, e.g., TiO<sub>2</sub> or Nb<sub>2</sub>O<sub>5</sub>, have a high activity in comparison to the conventional supports, e.g., Al<sub>2</sub>O<sub>3</sub> or SiO<sub>2</sub> [8,9]. This promoting effect of the reducible supports has been attributed to the creation of new active sites at the metal–support interface, which orig-

inates from the migration of support suboxide species onto the metal surface [10]. Arakawa et al. [11] have reported that the methanol synthesis from CO<sub>2</sub> hydrogenation over Cu/TiO<sub>2</sub> showed high turnover frequency because the rate of formate hydrogenation was enhanced by the synergetic effect between Cu and TiO<sub>2</sub>.

But titania presents the disadvantage of a low surface area ( $S_g \approx 50 \text{ m}^2/\text{g}$ ) and poor thermal stability as compared to its alumina counterparts ( $S_g \approx 200 \text{ m}^2/\text{g}$ ). The alumina–titania mixed oxide support appears very attractive to improve the mechanical strength, thermal stability and surface area of TiO<sub>2</sub>.

To date there have been no reports on the characterization of Cu-based catalysts supported on titanium-modified  $\gamma$ -Al<sub>2</sub>O<sub>3</sub> and their activity for CO<sub>2</sub> hydrogenation. It seems interesting to study the changes that occur in the nature of the support upon changing from  $\gamma$ -Al<sub>2</sub>O<sub>3</sub> to  $\gamma$ -Al<sub>2</sub>O<sub>3</sub>-TiO<sub>2</sub> mixed oxide supports with various amount of titanium, and the activity for CO<sub>2</sub> hydrogenation.

In this paper we will present characterization by different techniques for a series of 12 wt% copper catalysts supported on  $\gamma$ -Al<sub>2</sub>O<sub>3</sub> and three  $\gamma$ -Al<sub>2</sub>O<sub>3</sub>-TiO<sub>2</sub> supports with different TiO<sub>2</sub> content, prepared by impregnation methods. The activity and selectivity to methanol over Cu/ $\gamma$ -Al<sub>2</sub>O<sub>3</sub>-TiO<sub>2</sub> from CO<sub>2</sub> hydrogenation is also investigated.

## 2. Experimental

### 2.1. Catalysts preparation

A non-aqueous solution of titanium isopropoxide in ethanol was added to dry  $\gamma$ -alumina ( $\gamma$ -Al<sub>2</sub>O<sub>3</sub>, 20–40 mesh)

\* To whom correspondence should be addressed.

and kept under argon atmosphere for 24 h. The solids were washed with ethanol before drying, dried at 393 K and calcined at air flow at 773 K for 5 h. The solids prepared were named Al-Ti( $x$ ), where  $x = 100 \times n(\text{Ti})/(n(\text{Ti}) + n(\text{Al}))$ .

A series of copper catalysts containing 12 wt% Cu were prepared by impregnating the above supports using the appropriate amount of an aqueous solution of  $\text{Cu}(\text{NO}_3)_2$ . The impregnated samples were dried at 373 K and later calcined at 673 K for 4 h; hereafter the catalysts will be referred to as Cu/Al-Ti( $x$ ).

## 2.2. Catalytic reaction

Catalytic activity measurements were carried out by using a high-pressure microreactor (MRC8004) after introducing pretreatment gas ( $\text{H}_2$ ) at 300 °C for 3 h. The reactant gas was passed through the catalyst bed (2 ml, 20–40 mesh) under a total pressure of 3.0 MPa and a space velocity of  $3600 \text{ h}^{-1}$ , at certain temperature. The tubing from the catalyst bed to the gas chromatograph was heated at 393 K so as to avoid any condensation of the products. All experimental data were obtained under steady-state conditions that were usually maintained for several hours before changing the reaction temperature to obtain another set of data. The products were analyzed by an on-line gas chromatograph with a thermal detector, in which two parallel connected columns, Porapak-Q and TDX-01, were used to separate reaction products.

## 2.3. Temperature-programmed reduction (TPR)

TPR measurements were made in a flow system. 10 mg catalyst was pretreated in air at 400 °C and placed in a TPR cell at room temperature, into which  $\text{H}_2$ - $\text{N}_2$  (5:95) mixed gas was introduced. The water produced by the reduction was trapped on a 5A molecular sieve. The temperature of the sample was programmed to rise at a constant rate of 10 °C/min and the amount of  $\text{H}_2$  uptake during the reduction was measured by a thermal conductivity detector (TCD).

## 2.4. X-ray powder diffraction (XRD) experiments

Measurement of X-ray powder diffraction (XRD) was conducted by using a Rigaku D/Max-B for analysis of the crystal phase.

# 3. Results and discussion

## 3.1. XRD of calcined catalysts

Figure 1 displays the XRD patterns of titanium-modified alumina (Al-Ti( $x$ );  $x = 5, 10$  and  $15$ ). From figure 1, the pattern of the titanium-modified alumina ( $x = 5$ ) only displays wide peaks corresponding to the (400) and (440) planes of the support  $\gamma\text{-Al}_2\text{O}_3$  ( $2\theta = 46^\circ$  and  $67^\circ$ , respectively). With increasing Ti content, the phase of  $\text{TiO}_2$  crystallite appears. These results confirm that the catalysts with

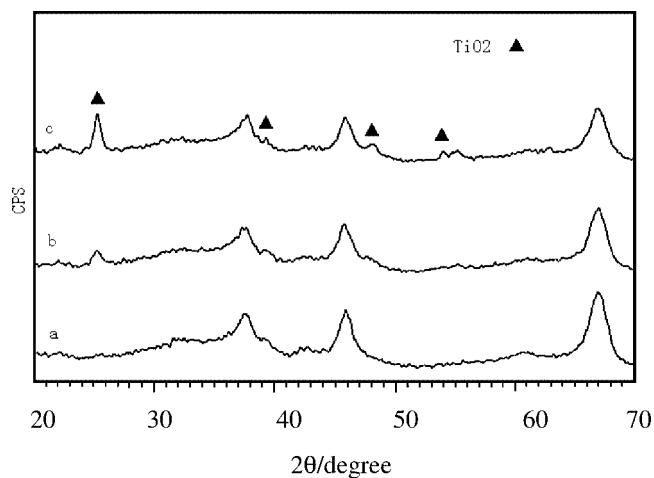


Figure 1. XRD profiles of  $\gamma\text{-Al}_2\text{O}_3$  with different Ti loading (a) Al-Ti(5), (b) Al-Ti(10) and (c) Al-Ti(15).

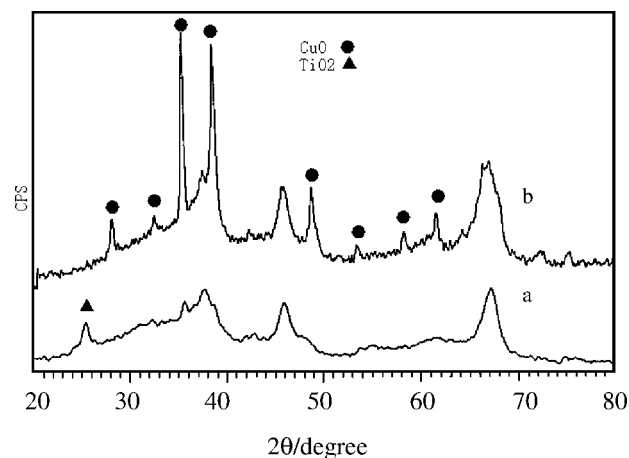


Figure 2. XRD profiles of  $\text{CuO}/\gamma\text{-Al}_2\text{O}_3$  and  $\text{CuO}/\text{Al-Ti}(10)$  catalysts: (a)  $12\text{CuO}/\text{Al-Ti}(10)$  and (b)  $12\text{CuO}/\gamma\text{-Al}_2\text{O}_3$ .

lower titanium contents (up to 10%) did not exhibit  $\text{TiO}_2$  crystallites.

The XRD patterns of the Cu catalysts supported on  $\gamma\text{-Al}_2\text{O}_3$  and titanium-modified  $\gamma\text{-Al}_2\text{O}_3$  are shown in figure 2. For the Cu/Al-Ti(10) catalyst, the diffraction peaks of CuO were broadened remarkably. In contrast to the CuO/Al-Ti(10) catalyst, the CuO/ $\gamma\text{-Al}_2\text{O}_3$  showed much narrower and sharper diffraction and two resolvable peaks at  $2\theta = 35^\circ$  and  $38^\circ$ , respectively. The results show that the adding of Ti had a significant influence on the particle size distribution and the structure of the catalyst. The copper oxide, titania and  $\gamma$ -alumina phases were present in an amorphous-like or microcrystalline state in the ternary catalysts.

## 3.2. XRD of reduced catalysts

When the ternary Cu/Al-Ti( $x$ ) catalysts were reduced by  $\text{H}_2$  at 300 °C, XRD lines (figure 3) for CuO were absent for the reduced samples while diffraction lines for  $\text{Cu}^0$  were present. This indicated that CuO in the ternary Cu/Al-

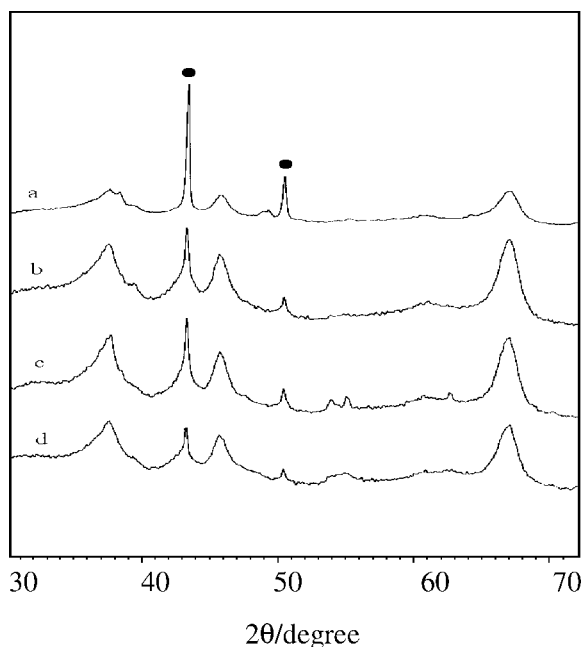


Figure 3. XRD profiles of reduced catalysts: (a) 12Cu/ $\gamma$ -Al<sub>2</sub>O<sub>3</sub>, (b) 12Cu/Al-Ti(5), (c) 12Cu/Al-Ti(10) and (d) 12Cu/Al-Ti(15); Cu (●).

Table 1  
Properties of reduced catalysts.

Catalyst	Metallic copper particles size <sup>a</sup> (nm)		Metallic copper area (XRD) <sup>b</sup> (m <sup>2</sup> /g <sub>cat</sub> )
12Cu/ $\gamma$ -Al <sub>2</sub> O <sub>3</sub>	52.43		0.28
12Cu/Al-Ti(5)	22.95 <sup>1</sup>	9.31 <sup>2</sup>	1.60
12Cu/Al-Ti(10)	20.00 <sup>1</sup>	4.04 <sup>2</sup>	2.08
12Cu/Al-Ti(15)	18.96 <sup>1</sup>	3.05 <sup>2</sup>	2.81

<sup>a</sup> 1 and 2 refer to particle size.

<sup>b</sup> Specific surface area of metallic copper calculated from XRD.

Ti(x) catalyst was completely reduced to metallic copper. The mean crystallite size was determined using the Scherrer equation,  $d = \kappa\lambda/\beta \cos \theta$  and the results are listed in table 1. This shows that the crystallite size of Cu decreases with the increasing of the content of TiO<sub>2</sub>. It is consistent with the XRD results of calcined and reduced catalysts. Furthermore, it is obvious that there exist two kinds of metallic copper particles with different crystallite size on the reduced CuO/Al-Ti(x) catalysts.

### 3.3. TPR

The TPR profiles of the catalysts are displayed in figure 4. Two reduction peaks can be observed in the TPR patterns of CuO/ $\gamma$ -Al<sub>2</sub>O<sub>3</sub>. According to Dow et al. [12], the low-temperature peak (assigned as  $\alpha$ ) is due to the reduction of the highly dispersed copper oxide species. The high-temperature peak (assigned as  $\beta$ ) has been ascribed to the reduction of bulk-like CuO phases. On the other hand, the CuO/Al-Ti(10) shows four peaks. The four peaks are designated by  $\alpha_1$ ,  $\alpha_2$ ,  $\beta_1$  and  $\beta_2$  in figure 4. The positions of peaks shift to lower temperature in comparison with the

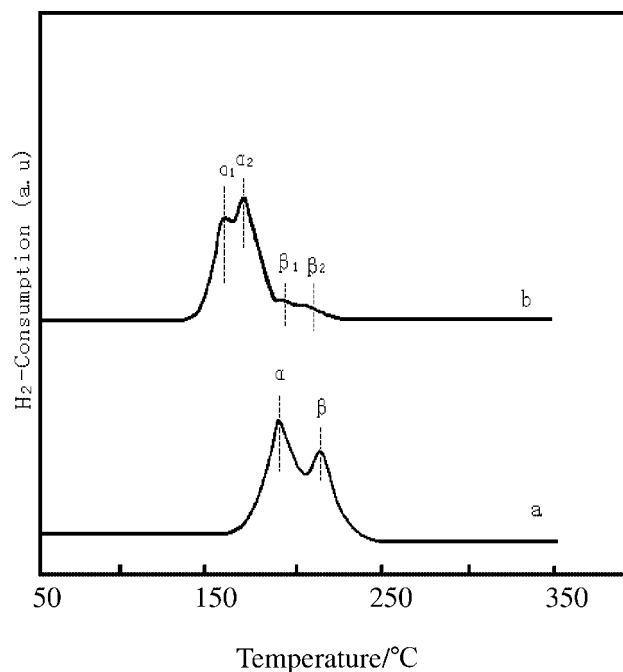


Figure 4. TPR profiles of 12CuO/ $\gamma$ -Al<sub>2</sub>O<sub>3</sub> and 12CuO/Al-Ti(10): (a) CuO/ $\gamma$ -Al<sub>2</sub>O<sub>3</sub> and (b) CuO/Al-Ti(10).

CuO/ $\gamma$ -Al<sub>2</sub>O<sub>3</sub> sample. It is well known that TiO<sub>2</sub> is partially reduced to TiO<sub>2-x</sub> under hydrogen at high temperature (above 500 °C) [13]. So the four TPR peaks on the CuO/Al<sub>2</sub>O<sub>3</sub>-TiO<sub>2</sub> catalyst are contributed to the reduction of CuO species. From figure 4, it can be seen that the reduction behavior of the CuO/Al-Ti(x) catalyst is thus obviously different from that of the CuO/ $\gamma$ -Al<sub>2</sub>O<sub>3</sub> catalyst. Adding of Ti decreases obviously the area of the high-temperature peak ( $\beta_1$  and  $\beta_2$ ) but enhances the area of the lower temperature peak ( $\alpha_1$  and  $\alpha_2$ ). Comparing the XRD (figure 2) and TPR results, we believe that the lower temperature TPR peak ( $\alpha_1$  and  $\alpha_2$ ) is contributed to reduction of the dispersed copper oxide, while the high-temperature TPR peak ( $\beta_1$  and  $\beta_2$ ) is the reduction of bulk CuO with different particle size which can be found in table 1. Deo et al. [14] reported that bridged-bonded vanadium oxide, such as Zr-O-V, is more reducible than that with terminal-bonded oxygen (V=O). Dow and Huang [15] have reported that when copper oxide is supported on YSZ (Y<sub>2</sub>O<sub>3</sub>-stabilized ZrO<sub>2</sub>), the interfacial oxygen ion of copper oxide can be removed at very low temperature to form third and fourth TPR peaks, i.e.,  $\alpha_1$  and  $\alpha_2$  peaks as well as  $\beta$  and  $\gamma$  peaks. Two TPR peaks with lower temperatures (namely  $\alpha_1$  and  $\alpha_2$ ) have been attributed to the hydrogen uptake of nested oxygen ions and temptable oxygen ions, respectively. The strong affinity between the surface oxygen vacancy ion of YSZ and the interface-boundary terminal oxygen ion of copper oxides will cause this Cu=O bond to become weakened. Dow and Huang designated these oxygen ions as nested oxygen ions. The interface-boundary terminal oxygen ions which are in the vicinity of the surface oxygen vacancy of YSZ are temptable oxygen ions. The nested oxygen ions and temptable oxygen ions are interface-boundary terminal oxygen ions of the sup-

ported copper oxide but have different environment and interaction with the surface oxygen vacancies of the YSZ support. We believe that  $\alpha_1$  and  $\alpha_2$  peaks of our CuO/Al–Ti(10) catalyst correspond to the  $\alpha_1$  and  $\alpha_2$  peaks of the CuO/YSZ catalyst in the literature [15]. From the result mentioned above, it can be found that the addition of Ti enhances the dispersion of CuO and promotes the reduction of CuO.

### 3.4. Effect of the composition and copper area of the catalyst on the catalytic activity

The catalytic activity and selectivity results obtained in a microreactor (MRC8004) are shown in figure 5. Carbon monoxide and methanol are the only carbon-containing products found under the reaction conditions ( $T = 180^\circ\text{C}$ ,  $P = 3.0\text{ MPa}$ ,  $\text{GHSV} = 3600\text{ h}^{-1}$ ,  $\text{H}_2/\text{CO}_2 = 3/1$ ). Comparing the Cu/Al–Ti( $x$ ) ternary catalysts with the binary Cu/ $\gamma$ - $\text{Al}_2\text{O}_3$  catalysts, it can be found that the former shows a higher conversion of  $\text{CO}_2$  and higher yield of methanol. This can be attributed to the fine particle size of metallic copper and higher copper metal surface area in the ternary catalysts. From figure 5, it can be seen that although the  $\text{CO}_2$  conversion of Cu/ $\gamma$ - $\text{Al}_2\text{O}_3$  is 3.2%, the Cu/Al–Ti(10) is as high as 7.36%; the yield of methanol on the 12Cu/Al–Ti(10) (6.5%) is four times more than that on 12Cu/ $\gamma$ - $\text{Al}_2\text{O}_3$  (1.59%). The yield of methanol is in the order of Cu/Al–Ti(10) > Cu/Al–Ti(15) > Cu/Al–Ti(5) > Cu/ $\text{Al}_2\text{O}_3$ .

Various compositions and different preparation methods of Cu-containing catalysts can strongly influence their catalytic activity for methanol synthesis. It has been proposed [16–19] that the yield of methanol is directly proportional to the surface of metallic copper for Cu/ZnO/ $\text{Al}_2\text{O}_3$  or supported copper catalysts in the synthesis of methanol from the hydrogenation of CO or  $\text{CO}_2$ . However, there are also conflicting reports [20–22] which suggest that the yield of methanol is not proportional to the surface area of metallic copper for the Cu/ZnO and Cu/ZnO/ $\text{Al}_2\text{O}_3$  catalysts. There are few studies on the relations of the catalytic activity for methanol synthesis from  $\text{CO}_2$  hydrogenation to the surface area of metallic copper.

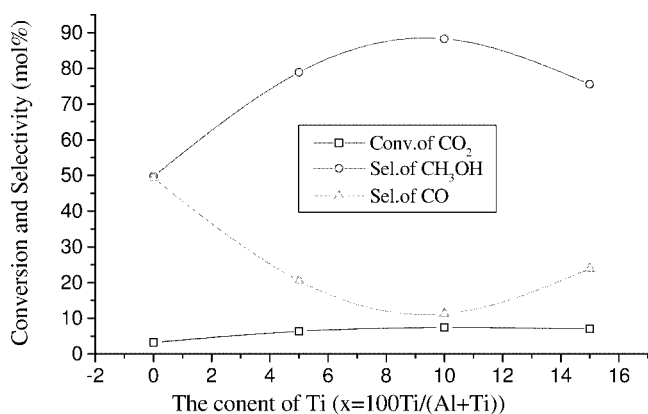


Figure 5. Effect of Ti content of the catalyst on  $\text{CO}_2$  hydrogenation. Reaction conditions:  $T = 180^\circ\text{C}$ ,  $P = 3.0\text{ MPa}$ ,  $\text{GHSV} = 3600\text{ h}^{-1}$ ,  $\text{CO}_2/\text{H}_2 = 1/3$  (molar ratio).

In our experiment, the effect of the surface area of metallic copper on the activity of synthesis of methanol from  $\text{CO}_2$  hydrogenation over Cu/Al–Ti( $x$ ) was studied and the results are shown in figure 6. It can be seen that the catalytic activity increased with the increase of the surface area of metallic copper, but it was not a linear relationship. This indicates that the catalytic activity of the catalysts depends on both the metallic copper surface area and the powerful synergy between copper and titanium dioxide, which is consistent with the result reported by Arakawa et al. [11].

### 3.5. Effect of reaction condition on catalytic behavior

The activity of the 12Cu/Al–Ti(10) catalyst for methanol synthesis with different temperature is shown in figure 7. It reveals that the yield of methanol has a maximum. It is well known that the rate of reaction increases with the increase of temperature kinetically, so the yield of methanol should increase with the increase of temperature. However, the yield of methanol declines with the increasing temperature because of the limitation of the thermodynamic equilibrium. Therefore, it can be concluded that the control factor

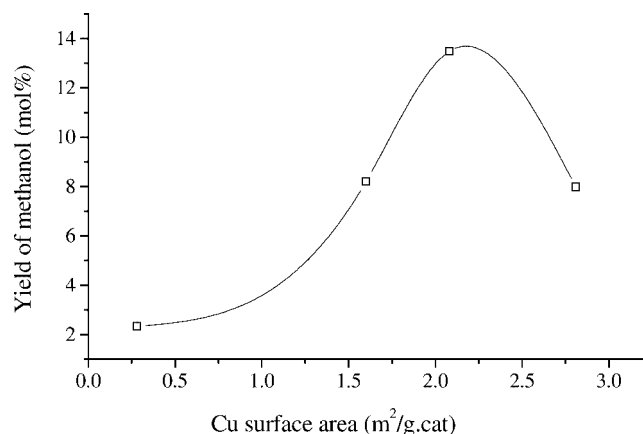


Figure 6. The relationship between the yield of methanol and Cu surface area at  $240^\circ\text{C}$ ,  $3.0\text{ MPa}$  and hourly space velocity of  $3600\text{ h}^{-1}$ .

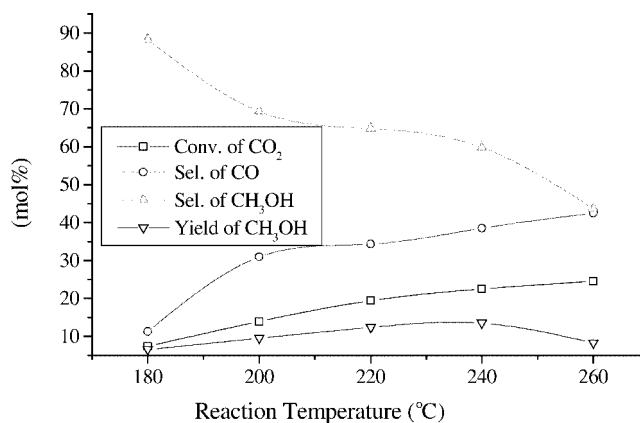
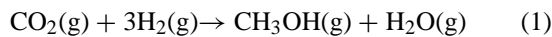


Figure 7. Effect of temperature on the catalytic activity of methanol synthesis at  $3.0\text{ MPa}$ , space velocity of  $3600\text{ h}^{-1}$  on 12Cu/Al–Ti(10) catalyst. Reaction conditions:  $P = 3.0\text{ MPa}$ ,  $\text{GHSV} = 3600\text{ h}^{-1}$ ,  $\text{CO}_2/\text{H}_2 = 1/3$  (molar ratio).

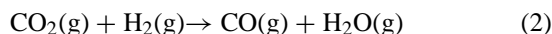
of the reaction transforms from kinetics to thermodynamics. From figure 7, it can be seen that the maximum is obtained at 240 °C.

In order to clarify whether methanol is produced directly by carbon dioxide hydrogenation or via the intermediate formation of carbon monoxide, the influence of the contact time on the methanol selectivity was investigated (as shown in figure 8). It is well known that the reverse water–gas-shift reaction (RWGS) and methanol synthesis reaction coexist in carbon dioxide hydrogenation presented as



$$\Delta H_{298} = -49.47 \text{ kJ/mol},$$

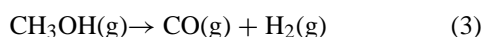
$$\Delta G_{298} = 3.30 \text{ kJ/mol},$$



$$\Delta H_{298} = -41.17 \text{ kJ/mol},$$

$$\Delta G_{298} = 28.64 \text{ kJ/mol}.$$

Carbon monoxide is an unavoidable intermediate precursor. If the catalyst is highly active and the contact time of reaction gas with the catalyst is long enough, the decomposition of methanol (produced in reaction (1)) or the hydrogenation of carbon monoxide (produced in reaction (2)) will take place. The possible secondary reaction is



$$\Delta H_{298} = 90.64 \text{ kJ/mol},$$

$$\Delta G_{298} = 25.34 \text{ kJ/mol}.$$

The selectivity of methanol ( $S$ ) and relative selectivity ( $\kappa$ ) are presented in figure 8 as functions of the contact time ( $\tau$ ) for 12Cu/Al–Ti(10). Both curves tend toward the finite values as the contact time approaches zero, suggesting that parallel routes to methanol and carbon monoxide exist under enough high hourly space velocity condition. However, it is noted that the selectivity to methanol increases and selectivity to carbon monoxide decreases with the increase of space velocity. It is well known that, if both carbon monox-

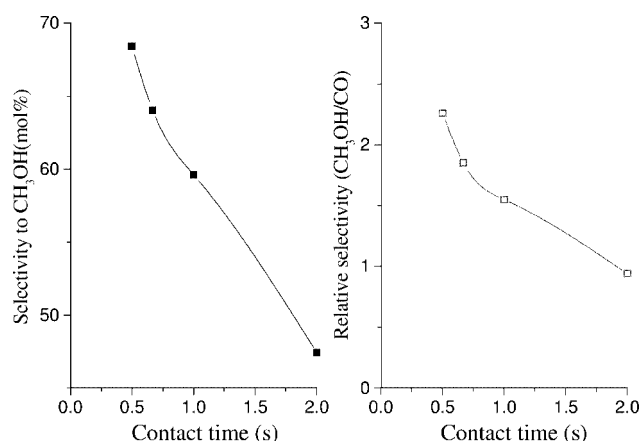


Figure 8. Effect of contact time on selectivity to methanol and relative selectivity on  $\text{CO}_2$  hydrogenation. Relative selectivity:  $\kappa = \chi(\text{CH}_3\text{OH})/\chi(\text{CO})$  ( $\chi$  = molar fraction). Reaction conditions:  $T = 240^\circ\text{C}$ ,  $P = 3.0 \text{ MPa}$ ,  $\text{CO}_2/\text{H}_2 = 1/3$  (molar ratio).

ide and methanol are formed merely from primary reaction simultaneously, the ratio of selectivity to methanol and carbon monoxide will remain constant with the change of the space velocity. The decreasing of selectivity to methanol and the increasing of that to carbon monoxide with the decreasing of the space velocity indicates that part of the carbon monoxide is formed from the secondary reaction under our experimental conditions. This is because when the gas hourly space velocity is low (or the contact time of reaction gas with the catalyst surface is long), secondary reaction of methanol decomposition or hydrogenation of carbon dioxide (reaction (3)) becomes an innegligible process. The increasing of selectivity to CO indicated that the methanol decomposition could be a major secondary reaction. As a result, the decreasing of selectivity to methanol and the increasing of that to CO were found with the decreasing of the gas hourly space velocity. In other words, only methanol and CO were primary products when the gas hourly space velocity was high enough; the contact time of reaction gas with the catalyst surface was short enough and all of the secondary process were depressed completely. This indicates that methanol and CO can be formed via reactions (1) and (2) simultaneously. From the analysis above, it can be concluded that the formation of methanol is a primary process of reaction (1). The methanol formation from hydrogenation of carbon monoxide (reaction (3)) formed from the reverse water–gas-shift reaction is negligible. From radiotracer studies using a Cu/ZnO/Al<sub>2</sub>O<sub>3</sub> catalyst under industrial conditions, Chinchén et al. [23] suggested that methanol synthesis proceeded from carbon dioxide, even in the presence of carbon monoxide. Koeppel and Baiker [24] conclude from the investigation of the influence of the residence time on the relative rate of product formation (CH<sub>3</sub>OH and CO) using Cu/ZrO<sub>2</sub> catalyst that methanol is formed from carbon dioxide via a reaction pathway parallel to that of the formation of carbon monoxide. These conclusions are basically consistent with ours.

#### 4. Conclusion

Cu/ $\gamma$ -Al<sub>2</sub>O<sub>3</sub>–TiO<sub>2</sub> catalysts with fine particles and high activity for synthesis of methanol from CO<sub>2</sub> hydrogenation have been prepared by the conventional impregnation method. The addition of TiO<sub>2</sub> leads to a decrease in crystallite sizes of the catalyst and made the copper in the catalyst exhibit amorphous-like or less well-ordered structure features. The optimized composition is  $n(\text{Ti})/(n(\text{Ti}) + n(\text{Al})) = 0.1$ . The catalytic activity increases with increasing copper surface area, but it is not a linear relationship. This indicates that a synergy for the synthesis of methanol exists between copper and titanium dioxide. The selectivity of methanol increases with the increase of space velocity, suggesting that methanol is the primary product and is formed directly from CO<sub>2</sub>/H<sub>2</sub>. The secondary process of hydrogenation of carbon monoxide via the route of the reverse water–gas-shift reaction is not significant for methanol synthesis from CO<sub>2</sub> hydrogenation.

## Acknowledgement

This research project was supported by the Zhejiang provincial Natural Science Foundation of China.

## References

- [1] G.C. Chinchin, P.J. Denny, J.R. Jennings, M.S. Spencer and K.C. Waugh, *Appl. Catal.* 36 (1988) 1.
- [2] R.A. Koppel and A. Baiker, *Appl. Catal.* 84 (1992) 77.
- [3] M. Satio, T. Fujitani, M. Takeuchi and T. Watanabe, *Appl. Catal.* 138 (1996) 311.
- [4] J.A. Brown, N. Homs and A.T. Bell, *J. Catal.* 124 (1990) 73.
- [5] J.S. Lee, K. Moon, S.H. Lee, S.Y. Lee and Y.G. Kim, *Catal. Lett.* 34 (1995) 93.
- [6] C. Frohlich, R.A. Koppel, A. Baiker, M. Kilo and A. Wokaun, *Appl. Catal.* 106 (1993) 275.
- [7] J.F. Deng, Q. Sun, Y.L. Zhang, D. Wu and S.Y. Chen, *Appl. Catal.* 139 (1996) 75.
- [8] M.R. Prairie, A. Renken and K.R. Thampi, *J. Catal.* 149 (1991) 131.
- [9] A. Boffa, C. Lin, A.T. Bell and G.A. Somorjai, *J. Catal.* 149 (1994) 149.
- [10] M.A. Vannice and C. Sudhakar, *J. Phys. Chem.* 88 (1984) 2429.
- [11] K.K. Bando, K. Sayama, H. Kusama, K. Okabe and H. Arakawa, *Appl. Catal.* 165 (1997) 391.
- [12] W.-P. Dow, Y.-P. Wang and T.-J. Huang, *Appl. Catal.* 190 (2000) 25.
- [13] B.A. Sexton, A.E. Hughes and K. Fogar, *J. Catal.* 77 (1982) 85.
- [14] G. Deo and I.E. Wachs, *J. Catal.* 146 (1994) 323.
- [15] W.-P. Dow, Y.-P. Wang and T.-J. Huang, *J. Catal.* 160 (1996) 155.
- [16] G.C. Chinchin, K.C. Waugh and D.A. Whan, *Appl. Catal.* 25 (1986) 101.
- [17] B. Denise, R.P.A. Sneeden, B. Beguin and O. Cherifi, *Appl. Catal.* 30 (1987) 353.
- [18] G.C. Chinchin and K.C. Waugh, *J. Catal.* 97 (1986) 280.
- [19] T.H. Fleisch and R.L. Mieville, *J. Catal.* 90 (1984) 165.
- [20] K. Klier, V. Chatikavanij, R.G. Herman and G.W. Simmons, *J. Catal.* 74 (1982) 343.
- [21] R. Burch and R.J. Chappel, *Appl. Catal.* 45 (1992) 65.
- [22] H. Berndt, V. Briehn and S. Evert, *Appl. Catal. B* 86 (1992) 65.
- [23] G.C. Chinchin, P.J. Denny, D.G. Parker, M.S. Spencer and D.A. Whan, *Appl. Catal.* 30 (1987) 333.
- [24] R.A. Koppel and A. Baiker, *Appl. Catal.* 84 (1992) 77.